 CMES, vol.88, no.4, pp.245-267, 2012

Robust Numerical Scheme for Singularly Perturbed Parabolic Initial-Boundary-Value Problems on Equidistributed Mesh

Srinivasan Natesan[1] **and S. Gowrisankar**[2]

Abstract: In this article, we propose a parameter-uniform computational technique to solve singularly perturbed parabolic initial-boundary-value problems exhibiting parabolic layers. The domain is discretized with a uniform mesh on the time direction and a nonuniform mesh obtained via equidistribution of a monitor function for the spatial variable. The numerical scheme consists of the implicit-Euler scheme for the time derivative and the classical central difference scheme for the spatial derivative. Truncation error, and stability analysis are carried out. Error estimates are derived, and numerical examples are presented.

Keywords: Singularly perturbed parabolic problem; Boundary layers; Adaptive mesh; Uniform convergence; Equidistribution mesh.

1 Introduction

Consider the singularly perturbed parabolic initial-boundary value problem (IBVP) in the domain $\Omega = (0,1) \times (0,T]$:

$$\begin{cases} u_t(x,t) + \mathcal{L}_\varepsilon u(x,t) = f(x,t), \quad (x,t) \in \Omega \\ u(x,0) = s(x), \quad \text{on } S_x = \{(x,0) : 0 \le x \le 1\}, \\ u(0,t) = a_0(t), \quad \text{on } S_0 = \{(0,t) : 0 \le t \le T\}, \\ u(1,t) = a_1(t), \quad \text{on } S_1 = \{(0,t) : 0 \le t \le T\}, \end{cases} \tag{1}$$

where

$$\mathcal{L}_\varepsilon u(x,t) \equiv -\varepsilon u_{xx}(x,t) + b(x)u(x,t),$$

[1] Department of Mathematics, Indian Institute of Technology Guwahati, Guwahati - 781 039, India.
[2] Department of Mathematics, Indian Institute of Technology Guwahati, Guwahati - 781 039, India.

$0 < \varepsilon \ll 1$ is a small parameter, and b, f are sufficiently smooth functions with $b(x) \geq \beta > 0$ on $0 \leq x \leq 1$. Under suitable continuity and compatibility conditions on the data, the IBVP (1) has a unique solution $u(x,t)$. Boundary layers occur in the solution when $\varepsilon \to 0$. These boundary layers are neighbors of the boundaries of the domain, where the solution varies rapidly, while away from the layers the solution changes slowly, and smoothly. Away from any corner of the domain a boundary layer of either regular or parabolic type may occur. A boundary layer is said to be of parabolic type, if the characteristics of the reduced equation corresponding to $\varepsilon = 0$ are parallel to the boundary, and of regular type, if these characteristics are not parallel to the boundary. A boundary layer near to a corner is said to be of corner type. These types of problems include the linearized Burgers' equation which arises in oil reservoir simulation Ewing (1983).

Numerical treatment of the IBVP (1) is difficult because of the presence of boundary layers in its solution. In particular, classical finite difference methods fail to yield satisfactory numerical results on uniform meshes, and to obtain stability one has to reduce the spatial step-size in relation with ε. The same is true for finite element methods in the case of uniform mesh and polynomial basis functions. Basically, by these methods one cannot obtain ε-uniform error estimates. When regular layers are present it is possible to obtain an ε-uniform method by constructing an appropriately fitted finite difference operator (*i.e.,* finite difference scheme with fitting factor) on uniform meshes. Indeed, Shishkin (1989) proved that this approach is not possible if a parabolic boundary layer is present, more details can be obtained from the book of Miller, O'Riordan and Shishkin (1996). One can also refer the books of Farrell, Hegarty, Miller, O'Riordan and Shishkin (2000), and Roos, Stynes and Tobiska (2006) for further results related to the theory and numerics of singularly perturbed parabolic problems.

The main goal of this paper is to provide an ε-uniform numerical method for the IBVP (1) with adaptive mesh. We obtain the adaptive mesh through the idea of equidistribution of singular component of $u(x,t)$ at some fixed time T_0, $0 < T_0 \leq T$, because the problem (1) exhibits boundary layers along boundary which do not have any effect on time. One can also refer Beckett and Mackenzie (2001) and Beckett and Mackenzie (2000) for the stationary problem where adaptive mesh applied. In this method, the time derivative is replaced by the backward difference scheme, and the spatial derivative is replaced by the central difference scheme. The proposed scheme is parameter-uniform convergent of order $O(\Delta t + N^{-2})$. Truncation errors are derived, stability analysis is carried out; and ε-uniform error estimates are obtained.

There are various numerical methods exist in the literature for singularly perturbed parabolic PDEs. To cite a few: Stynes and O'Riordan (1989) presented a uniformly

convergent finite element method for these types of problems using exponential basis functions. In Guo and Stynes (1993), finite element method of exponentially fitted lumped schemes were given. Farrell, Hemker and Shishkin (1996) proposed numerical methods for IBVPs of the form (1). The authors proposed two higher-order time accurate schemes for the parabolic IBVP (1) in Dep and Natesan (2009). In Mukherjee and Natesan (2008), the author developed an efficient hybrid numerical scheme for singularly perturbed parabolic IBVPs with interior layer. Deb and Natesan (2008) used extrapolation technique for singularly perturbed coupled system and Liu (2006) proposed shooting method for singularly perturbed two point boundary value problem. These technique can be successfully applied to singularly perturbed PDEs some extent.

We organize the rest of the paper as follows: In Section 2, we provide a-priori bounds on the derivatives of the analytical solution via decomposition. Section 3 we introduces the implicit upwind finite difference scheme and also adaptive spacial mesh via. equidistribution principle. Moreover we present the detailed numerical algorithm in Section 3.3. Afterwards, we carry out the error analysis for the upwind scheme in Section 4 and prove the main theoretical result, i.e., the ε-uniform optimal error bounds of the implicit upwind scheme on the adaptive mesh. Section 5 describes application of present method for semilinear singularly perturbed parabolic PDEs. In Section 6, we present the numerical results for two linear and a semilinear test problems to validate the theoretical results. Finally in Section 7, we summarize the main conclusions.

Through out this paper C denotes a generic positive constant independent of ε, the meshes (x_i, t_j), and the step sizes $h_i, \Delta t$. The norm $||\cdot||$ denotes the supremum norm.

2 Analytical Behavior of the Solution

In this section, we present some bounds for the analytical solution $u(x,t)$ of (1) and its derivatives. The proof of the theorems and more details can be found in the article by Miller, O'Riordan, Shishkin and Sishkina (1998).

Theorem 2.1 *Assume that the coefficients of the parabolic PDE, and the initial and boundary conditions given in (1) are sufficiently smooth, and satisfy the necessary compatibility conditions stated in Theorem 3 of Miller, O'Riordan, Shishkin and Sishkina (1998). Then, the IBVP (1) has a unique solution* $u(x,t) \in \mathscr{C}^4_\lambda(\overline{\Omega})$, *where*

$$\mathscr{C}^4_\lambda(\overline{\Omega}) =$$

$$\left\{ u : \frac{\partial^{i+j} u}{\partial x^i \partial t^j} \in \mathscr{C}^0_\lambda(\overline{\Omega}), \text{for all non-negative integers } i,\ j \text{ with } 0 \le i+2j \le 4 \right\},$$

here $\mathscr{C}^0_\lambda(\overline{\Omega})$ is the set of Hölder continuous functions. Furthermore, the derivatives of the solution u satisfy, for all non-negative integers i, j, such that $0 \le i+2j \le 4$,

$$\left\| \frac{\partial^{i+j} u}{\partial x^i \partial t^j} \right\| \le C\varepsilon^{-i/2}. \tag{2}$$

Proof. The proof can be found in Miller, O'Riordan, Shishkin and Sishkina (1998). ■

We shall decompose the solution u as $u = v + w$, where v, w are respectively the smooth and singular components. The smooth part is further decomposed into $v = v_0 + \varepsilon v_1$, where

$$\begin{cases} (v_0)_t(x,t) + b(x)v_0(x,t) = f(x,t), & \Omega, \\ v_0(x,0) = s(x), & \text{on } S_x, \end{cases}$$

and

$$\begin{cases} (v_1)_t(x,t) + \mathcal{L}_\varepsilon v_1(x,t) = \dfrac{\partial^2 v_0}{\partial x^2}, & \Omega, \\ v_1(x,0) = 0, \quad \text{on } S_x, \\ v_1(0,t) = 0, \quad v_1(1,t) = 0, \quad \text{on } S_0, S_1. \end{cases}$$

Thus, v satisfies the following IBVP:

$$\begin{cases} v_t(x,t) + \mathcal{L}_\varepsilon v(x,t) = f, & \text{in } \Omega, \\ v(x,0) = s(x), & \text{on } S_x, \\ v(0,t) = v_0(0,t), \quad v(1,t) = v_0(1,t), & \text{on } S_0, S_1. \end{cases}$$

The singular component w is the solution of the IBVP

$$\begin{cases} w_t(x,t) + \mathcal{L}_\varepsilon w(x,t) = 0, & \text{in } \Omega, \\ w(x,0) = 0, & \text{on } S_x, \\ w(0,t) = a_0(t) - v_0(0,t), \quad w(1,t) = a_1(t) - v_0(1,t), & \text{on } S_0, S_1. \end{cases}$$

Further, we decompose the singular component w into left and right components as $w = w_\ell + w_r$, where w_ℓ and w_r respectively, satisfy the following problems:

$$\begin{cases} (w_\ell)_t(x,t) + \mathcal{L}_\varepsilon w_\ell(x,t) = 0, & \text{in } \Omega, \\ w_\ell(x,0) = 0, & \text{on } S_x, \\ w_\ell(0,t) = a_0(t) - v_0(0,t), \quad w_\ell(1,t) = 0, & \text{on } S_0, S_1, \end{cases}$$

and

$$\begin{cases} (w_r)_t(x,t)+\mathfrak{L}_\varepsilon w_r(x,t)=0, & \text{in } \Omega,\\ w_r(x,0)=0, & \text{on } S_x,\\ w_r(0,t)=0, \quad w_r(1,t)=a_1(t)-v_0(1,t), & \text{on } S_0,S_1. \end{cases}$$

The smooth and singular components v, and w satisfy the following bounds.

Theorem 2.2 *Miller, O'Riordan, Shishkin and Sishkina (1998) Let $u(x,t)$ be the solution of the IBVP (1). And assume that the coefficients of the parabolic PDE, and the initial and boundary conditions given in (1) are sufficiently smooth, and satisfy the necessary compatibility conditions. Then, for all non-negative integers $i,\ j$, such that $0 \le i+2j \le 4$, we have*

$$\left\| \frac{\partial^{i+j} v}{\partial x^i \partial t^j} \right\| \le C(1+\varepsilon^{1-i/2}), \quad \forall (x,t) \in \Omega,$$
$$\left| \frac{\partial^{i+j} w_\ell}{\partial x^i \partial t^j} \right| \le C\varepsilon^{-i/2} e^{-x/\sqrt{\varepsilon}}, \text{ and } \left| \frac{\partial^{i+j} w_r}{\partial x^i \partial t^j} \right| \le C\varepsilon^{-i/2} e^{-(1-x)/\sqrt{\varepsilon}}.$$

Proof. The proof can be found in Miller, O'Riordan, Shishkin and Sishkina (1998). ■

3 The Numerical Solution

In this section, we discretize the parabolic IBVP (1), the time derivative is replaced by the backward difference scheme, and the spatial derivative is replaced by the central difference scheme. Later, we introduce the equidistribution mesh, and derive the finite difference scheme (4). Finally, we provide the numerical algorithm to obtain the equidistributed mesh.

3.1 Finite Difference Scheme

On the time domain [0,T], we introduce the equidistant meshes with uniform time step Δt such that

$$S_t^M = \{t_n = n\Delta t,\ n = 0,\dots,M,\ \Delta t = T/M\},$$

where M denotes the number of mesh elements in the t-direction.

We consider the finite difference approximation of (1) on a non-uniform spatial discretization

$$\overline{\Omega}_x^N = \{0 = x_0 < x_1 < \cdots < x_N = 1\},$$

and denote the spatial step sizes by

$$h_i = x_i - x_{i-1}, \quad i = 1, \ldots, N.$$

Without loss of generality, we will assume that N is even. Before describing the scheme, for a given mesh function $v(x_i, t_n) = v_i^n$, define the forward and backward differences δ_x^+, δ_x^- in space by

$$\delta_x^+ v_i^n = \frac{v_{i+1}^n - v_i^n}{h_{i+1}}, \quad \delta_x^- v_i^n = \frac{v_i^n - v_{i-1}^n}{h_i},$$

respectively, the second-order finite difference operator δ_x^2 as

$$\delta_x^2 v_i^n = \frac{2(\delta_x^+ v_i^n - \delta_x^- v_i^n)}{h_i + h_{i+1}},$$

and define the backward difference operator δ_t in time by

$$\delta_t v_i^n = \frac{v_i^n - v_i^{n-1}}{\Delta t},$$

We discretise equation (1) by means of the backward Euler scheme for the time derivative, and the central difference for the space derivative. Hence the discretization of (1) takes the form

$$\begin{cases} \delta_t U_i^{n+1} + L_\varepsilon U_i^{n+1} = f(x_i, t_{n+1}), \quad \text{for } i = 1, \ldots, N-1, \\ U_0^{n+1} = a_0(t_{n+1}), \quad U_N^{n+1} = a_1(t_{n+1}), \\ U_i^0 = s(x_i), \quad \text{for } i = 1, \ldots, N-1, \end{cases} \tag{3}$$

where L_ε is the discretization of the differential operator $\mathcal{L}_\varepsilon$ using the central difference for the spatial derivative,

$$L_\varepsilon U_i^{n+1} = -\varepsilon \delta_x^2 U_i^{n+1} + b_i U_i^{n+1}.$$

After rearranging the terms in (3), we obtain the following form of the difference scheme:

$$\begin{cases} r_i^- U_{i-1}^{n+1} + r_i^c U_i^{n+1} + r_i^+ U_{i+1}^{n+1} = g_i^n, \quad \text{for } i = 1, \ldots, N-1, \\ U_0^{n+1} = a_0(t_{n+1}), \quad U_N^{n+1} = a_1(t_{n+1}), \\ U_i^0 = s(x_i), \quad \text{for } i = 1, \ldots, N-1, \end{cases} \tag{4}$$

where

$$r_i^- = \frac{-2\varepsilon\Delta t}{h_i(h_i+h_{i+1})}, \qquad r_i^+ = \frac{-2\varepsilon\Delta t}{h_{i+1}(h_i+h_{i+1})}, \qquad r_i^c = 1+\Delta t b_i - r_i^- - r_i^+,$$
$$b_i = b(x_i), \qquad g_i^n = U_i^n + \Delta t f(x_i, t_{n+1}).$$

To determine the value of the monitor function (8), we have to know the approximate value of the singular component $w(x,t)$. To calculate the numerical value W_i^n of $w(x_i,t_n)$, we use the numerical approximate value V_i^n of $v(x_i,t_n)$ from the following recurrence relation:

$$\begin{cases} (1+\Delta t b(x_i))V_i^{n+1} = V_i^n + \Delta t f(x_i,t_{n+1}), \quad \text{for } i = 1,\ldots,N, \\ V_i^0 = s(x_i). \end{cases} \tag{5}$$

3.2 Adaptive spatial mesh via. equidistribution

Since the solution $u(x,t)$ of the IBVP(1) exhibits boundary layers, one has to use layer-adapted nonuniform spatial mesh, which are fine inside the boundary layer region, and coarse in the outer region. To obtain such a mesh, we use the idea of equidistribution of a positive monitor function given in (8). Here we consider equidistribution of $u(x,t)$ at some fixed time T_0, $0 < T_0 \leq T$, because the problem (1) exhibits regular layer along the boundaries, which will not have any impact on the temporal component. Moreover we assume that $u(x,T_0)$ exhibit the layer phenomena. A mesh is said to be equidistributing $u(x,T_0)$, if

$$\int_{x_{i-1}}^{x_i} M(u(s,T_0),s)ds = \int_{x_i}^{x_{i+1}} M(u(s,T_0),s)ds, \quad i = 1,\ldots,N-1, \tag{6}$$

where $M(u(x,T_0),x)$ is a strictly positive, $\mathscr{L}_1$–integrable function. Equation (6) can also be written in the following form:

$$\int_{x_{i-1}}^{x_i} M(u(s,T_0),s)ds = \frac{1}{N}\int_0^1 M(u(s,T_0),s)ds, \quad i = 1,\ldots,N. \tag{7}$$

Here, we consider the following monitor function

$$M(u(x,T_0),x) = \alpha + |w_{xx}(x,T_0)|^{1/m}, \quad m \geq 2, \tag{8}$$

where α is a positive constant that is independent of N and $w(x,t)$ is the singular component of $u(x,t)$. One dimensional version of the monitor function (8) given by Beckett and Mackenzie (2000) impressed us to take

$$\alpha = \int_0^1 |w_{xx}(s,T_0)|^{1/m} ds. \tag{9}$$

The selection of this α will help to distribute the number mesh point inside and outside the boundary layer region equally. The effect of increasing m is to smooth the monitor function, which in turn leads to a smoother distribution of the mesh points. From Beckett and Mackenzie (2000), one can clearly see the influence of the parameter m. In all of our numerical experiments, we will take $m = 2$.

In order to compute the approximation of the monitor function at the ith interior node of the spatial mesh, M_i, we assume for some integer S($0 < S \leq M$) that $w(x_i, T_0) = W_i^S$, where $S\Delta t = T_0$,

$$M_i = \alpha_{dis} + |\delta_x^2 W_i^S|^{1/m}, \quad \text{for } i = 1, \ldots, N-1, \tag{10}$$

where $W_i^S = U_i^S - V_i^S$ and α_{dis} is the discrete form of (9), which can be written as

$$\alpha_{dis} = h_1 |\delta_x^2 W_1^S|^{1/m} + \sum_{i=2}^{N-1} h_i \left\{ \frac{|\delta_x^2 W_{i-1}^S|^{1/m} + |\delta_x^2 W_i^S|^{1/m}}{2} \right\} + h_N |\delta_x^2 W_{N-1}^S|^{1/m}.$$

For a truly adaptive algorithm, the monitor function has to be approximated from the numerical solution. For example, a simple discretization of (6) results in the set of equations

$$M_{i-1/2}(x_i - x_{i-1}) = M_{i+1/2}(x_{i+1} - x_i), \quad \text{for } i = 1, \ldots, N-1,$$

where $M_{i\pm 1/2}$ is an approximation to $M(u(x_{i\pm 1/2}, T_0), x_{i\pm 1/2})$.

The detailed numerical algorithm to obtain the equidistribution mesh is given in Section 3.3.

3.3 Numerical algorithm

To get the equidistribution gird and the corresponding numerical solution, we use the following algorithm:

1. Take $k = 0$. Take the uniform spatial mesh $\{x_i^{(0)}\}$ as the initial value for the iteration. Choose a constant $C > 1$ that controls when the algorithm has to be terminated.

2. Compute the discrete solution $\{U_i^{n,(k)}\}$ and $\{V_i^{n,(k)}\}$ satisfying (4) and (5), respectively with the help of the spatial mesh $\{x_i^{(k)}\}$.

3. Find the singular component of the discrete solution by $W_i^{n,(k)} = U_i^{n,(k)} - V_i^{n,(k)}$.

4. For a given mesh $\{x_i^{(k)}\}$ and the singular component of the discrete solution $\{W_i^{n,(k)}\}$, set

$$H_i^{(k)} = \left(\frac{M_{i-1}^{(k)} + M_i^{(k)}}{2} \right) (x_i^{(k)} - x_{i-1}^{(k)}), \quad \text{for } i = 1, \ldots, N,$$

where $M_i^{(k)}$ is calculated from (10), and set $M_0^{(k)} = M_1^{(k)}$ and $M_N^{(k)} = M_{N-1}^{(k)}$.

5. Set $L_0 = 0$ and $L_i = \sum_{j=1}^{i} H_j^{(k)}$ for $i = 1, \ldots, N$. Define

$$C^{(k)} := \frac{N}{L_N} \max_{i=0,1,\ldots,N} H_i^{(k)}.$$

6. If $C^{(k)} \leq C$, then go to Step 9.

7. Set $Y_i = iL_N/N$ for $i = 0, 1, \ldots, N$. Interpolate the points (L_i, x_i). Generate the new mesh $\{x_i^{(k+1)}\}$ by evaluating this interpolant at the Y_i for $i = 0, 1, \ldots, N$.

8. Set $k = k + 1$, return to Step 2.

9. Take $\{x_i^{(k)}\}$ as the final mesh and compute $U_i^{n,(k)}$ then stop.

4 Error Analysis

Here, we derive the truncation error for the numerical scheme, and carry out the stability analysis. Finally, we obtain the ε-uniform error estimate.

The following lemma provides the stability result for a general numerical scheme for the IBVP (1). The proof of this lemma can be found in the book of Roos, Stynes and Tobiska (2006). Here, we are only stating the result.

Lemma 4.1 *Consider the IBVP (1) and the difference scheme (3), the difference scheme (excluding the initial and boundary conditions) can be written as*

$$\delta_t U^{n+1} + L_\varepsilon U^{n+1} := AU^{n+1} - DU^n = F^n, \quad \text{for } n = 0, \cdots, M-1, \tag{11}$$

where $U^n = (U_1^n, \cdots, U_{N-1}^n)^T$, F^n is a vector independent of the computed solution, and A and D are matrices and also that A is an M-matrix, and $D \geq 0$.

Let y and z be two mesh functions, such that $y^n = (y_0^n, \cdots, y_N^n)^T$, and $z^n = (z_0^n, \cdots, z_N^n)^T$ for each n. Assume that $\left|\delta_t y^{n+1} + L_\varepsilon y^{n+1}\right| \leq \delta_t z^{n+1} + L_\varepsilon z^{n+1}$, for $n = 0, \cdots, M-1$, and $|y| \leq z$ on the boundary $S_x \cup S_0 \cup S_1$. Then, $|y| \leq z$ on $\overline{\Omega}_x^N \times S_t^M$.

Proof. The difference scheme (4) can be written in the form of (11) with $A = (a_{ij})$ and $D = (d_{ij})$ as

$$a_{i,i-1} = \frac{r_i^-}{\Delta t}, \quad a_{i,i} = \frac{r_i^c}{\Delta t}, \quad a_{i,i+1} = \frac{r_i^+}{\Delta t},$$
$$d_{i,i} = \frac{1}{\Delta t}.$$

A short calculation shows that the matrix A is an M-matrix and the matrix $D \geq 0$. Therefore, the difference scheme satisfies the hypotheses of Lemma 3.2, Roos, Stynes and Tobiska (2006) and immediately the required result follows. ∎

Corollary 4.2 *The difference scheme given in (4) satisfies the discrete maximum principle.*

From the Corollary 4.2 one can observe that the scheme (4) has a unique solution at each time level. Combining the maximum principle with a barrier function of the form $C(1+x)$, one obtains a priori bound

$$\max_{i,n} |U_i^n| \leq C||f|| \quad \text{for all } i,n. \tag{12}$$

Theorem 4.3 *Let u and U be respectively the continuous and the numerical solutions of the IBVPs (1), and (4). Then, we have the following bound*

$$\max_{i,n} |u(x_i,t_n) - U_i^n| \leq C[\Delta t + N^{-2}] \quad \textit{for all } i,n. \tag{13}$$

Proof. Let $\eta_i^n = u_i^n - U_i^n$ be the error in the computed solution at each mesh point (x_i,t_n). Write the scheme (3) as

$$\delta_t U_i^n + L_\varepsilon U_i^n = f_i^n \quad i = 1,\ldots,N-1, \quad n = 1,\ldots,M,$$

Then at each point $(x_i,t_n) \in \overline{\Omega}_x^N \times S_t^M$, the truncation error of the scheme is

$$\delta_t \eta_i^n + L_\varepsilon \eta_i^n = \chi_{1,i}^n + \chi_{2,i}^n,$$

where

$$\chi_{1,i}^n := L_\varepsilon U_i^n - (\mathcal{L}_\varepsilon u)_i^n \quad \text{and} \quad \chi_{2,i}^n := \delta_t u_i^n - (u_t)_i^n,$$

are the truncation errors for the space and time discretization, respectively.

Decompose η as $\eta = \phi + \psi$. Here the function ϕ_i^n is, for each fixed $n = 0, \ldots, M$, the solution of the discrete two-point boundary value problem

$$\begin{cases} L_\varepsilon \phi_i^n = \chi_{1;i}^n & \text{for } i = 1, \ldots, N-1, \\ \phi_0^n = \phi_N^n = 0, \end{cases} \tag{14}$$

while ψ_i^n, the solution of a discrete parabolic problem, is defined by

$$\begin{cases} \delta_t \psi_i^n + L_\varepsilon \psi_i^n = \chi_{2,i}^n - \delta_t \phi_i^n & \text{for } i = 1, \ldots, N-1, \\ \psi_0^n = \psi_N^n = 0 & \text{for } n = 1, \ldots, M, \\ \psi_i^0 = -\phi_i^0 & \text{for } i = 0, \ldots, N. \end{cases} \tag{15}$$

Equation (14) is precisely the identity one gets when analyzing the error ϕ in a two-point boundary value problem that has been discretized using L_ε, with $\chi_{1;i}^n$ playing the role of truncation error and can be bounded using technique from Beckett and Mackenzie (2001) and equation (2) with $j = 0$. The problem (1) exhibits regular boundary layers and the same is true for the equation (14) consequently the error bound derived in Beckett and Mackenzie (2001) can be invoked for all temporal level:

$$|\phi_i^n| \leq CN^{-2}, \quad \text{for all } i, n, \tag{16}$$

with the assumption that $N^{-1} \gg \sqrt{\varepsilon}$ and the fact that our problem exhibits regular boundary layers.

Next, consider the other error component ψ. Lemma 4.1 implies that the problem (15) satisfies a discrete maximum principle just as (3) does, so

$$\begin{aligned} \|\psi\| &= C\left(\max_i |\phi_i^0| + \|\chi_2 - \delta_t \phi\|\right), \\ &= C\left[N^{-2} + \Delta t + \|\delta_t \phi\|\right], \end{aligned} \tag{17}$$

where we used (16) with $n = 0$ and also

$$|\chi_{2,i}^n| \leq C\Delta t \quad \text{for } i = 1, \ldots, N-1 \text{ and } n = 1, \ldots, M,$$

which is easily verified using a Taylor expansion and (2). It remains to deal only with $\delta_t \phi$ in (17). Using the assumption that $b = b(x)$ is independent of t, a short calculation shows that for each fixed n, the definition (14) implies that $\delta_t \phi$ satisfies

$$\begin{aligned} L_\varepsilon (\delta_t \phi)_i^n = \delta_t \chi_{1,i}^n \quad & \text{for } i = 1, \ldots, N-1, \\ (\delta_t \phi)_0^n = (\delta_t \phi)_N^n = 0. & \end{aligned} \tag{18}$$

To analyze the discrete two-point boundary value problem (18), observe that

$$\begin{aligned}\delta_t \chi^n_{1,i} &= \frac{1}{\Delta t}\left(\chi^n_{1,i} - \chi^{n-1}_{1,i}\right),\\ &= \frac{1}{\Delta t}\left((L_\varepsilon u^n_i - (\pounds_\varepsilon u)^n_i) - (L_\varepsilon u^{n-1}_i - (\pounds_\varepsilon u)^{n-1}_i)\right),\\ &= \frac{1}{\Delta t}\left((L_\varepsilon u^n_i - L_\varepsilon u^{n-1}_i) - ((\pounds_\varepsilon u)^n_i - (\pounds_\varepsilon u)^{n-1}_i)\right).\end{aligned}$$

Let $\hat{\pounds}_\varepsilon u = -\varepsilon u_{xx}$ and $\hat{L}_\varepsilon u^n_i = -\varepsilon \delta_x^2 u^n_i$. That is, $\hat{L}_\varepsilon u$ is the discretization of $\pounds_\varepsilon u$. Then one can write the above formula as

$$\delta_t \chi^n_{1,i} = \frac{1}{\Delta t}\int_{t_{n-1}}^{t_n} [\hat{L}_\varepsilon u_t(x_i,t) - \hat{\pounds}_\varepsilon u_t(x_i,t)],$$

Hence, using the Peano kernel theorem as in Kellogg and Tsan (1978), one obtains same estimate on $\delta_t \chi^n_{1,i}$ as the corresponding truncation error bounds arising in Beckett and Mackenzie (2001) for a standard two-point reaction-diffusion boundary value problem, since the bounds of (2) are unaffected by the presence of an extra $t-$derivative.

This observation imply that (18) can be analyzed in the same way as (14), except that one uses the bound (2) with $j = 1$. We therefore obtain

$$|\delta_t \phi^n_i| \leq CN^{-2} \quad \text{for all } i,n. \tag{19}$$

Combining (16), (17) and (19), we get (13).

5 Semilinear singular perturbation parabolic problem

In this section, we consider the following quasilinear singular perturbation parabolic PDE of the form

$$\begin{cases} u_t - \varepsilon u_{xx} = b(x,t,u), \quad (x,t) \in G = \Omega \times (0,T] \equiv (0,1)\times(0,T],\\ u(x,0) = u_0(x), \quad x \in \Omega,\\ u(0,t) = u(1,t) = 0, \quad t \in (0,T], \end{cases} \tag{20}$$

where ε is small positive parameter. Under sufficient smoothness and compatibility conditions imposed on the functions $b(x,t,u)$ and $u_0(x)$ the parabolic problem (20) in general admits a unique solution $u(x,t)$ which exhibits boundary layers. For more information on existence and uniqueness one can refer Ladyženskaja, Solonnikov and Ural'ceva (1988).

To solve (20), we use the linearization process and obtain the Newton sequence $\{u^m\}$ for the initial guess u^0 satisfying the initial and boundary conditions of the problem. Thus we define u^{m+1} for each fixed m, to be the solution of the following linear parabolic IBVP,

$$\begin{cases} u_t^{m+1} - \varepsilon u_{xx}^{m+1} - b^m(x,t)u^{m+1} = f^m(x,t), \quad (x,t) \in G \\ u^{m+1}(x,0) = u_0(x), \quad 0 < x < 1, \\ u^{m+1}(0,t) = 0, \quad u^{m+1}(1,t) = 0, \quad 0 \le t \le T, \end{cases} \tag{21}$$

where $m \ge 0$ and $b^m(x,t)$ and $f^m(x,t)$ are given by

$$\begin{cases} b^m(x,t) = b_u(x,t,u^m), \\ f^m(x,t) = b(x,t,u^m) - b^m(x,t)u^m. \end{cases} \tag{22}$$

Hence for fixed m, we solve (21) using computation method discussed earlier. Moreover we assume that the problem admits regular boundary layers. Numerical results of (20) presented on the following section.

6 Numerical Results

In this section, we shall present the numerical results obtained by the fully discrete scheme (4) for two linear and a semilinear test problems on the rectangular mesh $\overline{G}_\varepsilon^{N,M} = \overline{\Omega}_x^N \times S_t^M$, where $\overline{\Omega}_x^N$ is the equidistribution mesh obtained from the numerical algorithm. In all the numerical experiments we will fix $m = 2$ and $T_0 = 1$, which is necessary to define the monitor function (8). Moreover in all the tables we begin with $N = 32$ and the time step $\Delta t = 0.1$ and we multiply N by two and divide Δt by four. The reason for dividing Δt by four is to highlight the spatial order of convergence properly.

Example 6.1 *Consider the following parabolic initial-boundary-value problem:*

$$u_t(x,t) - \varepsilon u_{xx}(x,t) + u(x,t) = f(x,t), \quad (x,t) \in (0,1) \times (0,1]. \tag{23}$$

The right-hand side source term, initial and boundary conditions are calculated from the exact solution

$$u(x,t) = \left(t + \frac{x^2}{2\varepsilon}\right) \operatorname{erfc}\left(\frac{x}{2\sqrt{\varepsilon t}}\right) - \sqrt{\frac{t}{\pi\varepsilon}}\, x e^{-x^2/4\varepsilon t},$$

where erfc is the complementary error function. As the exact solution of the problem (6.1) is known, for each ε, we calculate the maximum point-wise error by

$$e_\varepsilon^{N,\Delta t} = \max_{(x_i,t_n) \in \overline{G}_\varepsilon^{N,M}} |u(x_i,t_n) - U^{N,\Delta t}(x_i,t_n)|,$$

where $u(x_i,t_n)$ and $U^{N,\Delta t}(x_i,t_n)$ respectively, denote the exact and the numerical solution obtained on the mesh with N mesh intervals in the spatial direction and M mesh intervals in the $t-$direction such that $\Delta t = T/M$ is the uniform time step. In addition, we determine the corresponding order of convergence by

$$p_\varepsilon^{N,\Delta t} = \log_2 \left(\frac{e_\varepsilon^{N,\Delta t}}{e_\varepsilon^{2N,\Delta t/4}} \right).$$

The calculated maximum point-wise errors $e_\varepsilon^{N,\Delta t}$ and the corresponding order of convergence $p_\varepsilon^{N,\Delta t}$ for Example 6.1 are given in Table 1 and Table 2 respectively. From these results one can observe the ε–uniform first-order convergence of the numerical solution.

Further, we have calculated the normalized flux

$$F_\varepsilon u(x,t) = \sqrt{\varepsilon}\frac{\partial u(x,t)}{\partial x},$$

and its numerical approximation

$$F_\varepsilon^N U^{N,\Delta t}(x_i,t_n) = \sqrt{\varepsilon}\delta_x^+ U_i^n.$$

The errors in the normalized flux have been calculated as

$$r_\varepsilon^{N,\Delta t} = \max_{1\le n\le M} \|F_\varepsilon u(x_0,t_n) - F_\varepsilon^N U^{N,\Delta t}(x_0,t_n)\|,$$

and the rate of convergence is determined from

$$q_\varepsilon^{N,\Delta t} = \log_2 \left(\frac{r_\varepsilon^{N,\Delta t}}{r_\varepsilon^{2N,\Delta t/4}} \right).$$

The calculated maximum point-wise errors in the normalized flux $r_\varepsilon^{N,\Delta t}$ and the corresponding order of convergence $q_\varepsilon^{N,\Delta t}$ for Example 6.1 are given in Table 3 and Table 4. Again, one can see the ε–uniform convergence in Table 3, and the first-order convergence rate from Table 4. In Figures 1 (a) and (b), the maximum pointwise errors in the solution and the normalized flux are plotted respectively, which reflect the fact of first-order convergence independent of ε.

Example 6.2 *Consider the following parabolic initial-boundary value problem:*

$$\begin{cases} u_t - \varepsilon u_{xx} + \sqrt{x+1}u = 1, \quad (x,t) \in (0,1)\times(0,1], \\ u(x,0) = 0, \quad 0 < x < 1, \\ u(0,t) = 0, \quad u(1,t) = 0, \quad 0 \le t \le 1. \end{cases} \tag{24}$$

Table 1: *Maximum point-wise error of the solution* $e_{\varepsilon}^{N,\Delta t}$ *for Example* 6.1.

	Number of Intervals N					
ε	32	64	128	256	512	1024
10^{0}	8.3624e-03	2.6269e-03	7.1243e-04	1.8369e-04	4.6626e-05	1.1745e-05
10^{-2}	9.5404e-03	2.7104e-03	7.2159e-04	1.8606e-04	4.7251e-05	1.1905e-05
10^{-4}	9.5334e-03	2.7205e-03	7.3760e-04	1.8837e-04	4.7627e-05	1.1983e-05
10^{-6}	9.6177e-03	2.7165e-03	7.2577e-04	1.8717e-04	4.7525e-05	1.2266e-05
10^{-8}	9.6062e-03	2.7314e-03	7.2639e-04	1.8723e-04	4.7546e-05	1.1978e-05
10^{-10}	9.5997e-03	2.7503e-03	7.2762e-04	1.8755e-04	4.7532e-05	1.1980e-05

Table 2: *Rate of convergence of the solution* $p_{\varepsilon}^{N,\Delta t}$ *for Example* 6.1 .

	Number of Intervals N				
ε	32	64	128	256	512
10^{0}	1.6705	1.8826	1.9554	1.9781	1.9891
10^{-2}	1.8155	1.9093	1.9554	1.9773	1.9887
10^{-4}	1.8091	1.8829	1.9693	1.9837	1.9907
10^{-6}	1.8239	1.9042	1.9551	1.9776	1.9541
10^{-8}	1.8143	1.9108	1.9560	1.9774	1.9889
10^{-10}	1.8034	1.9183	1.9559	1.9803	1.9883

The numerical solution is plotted in Figures 2 (a) and (b) for $\varepsilon = 1e-1$ and $\varepsilon = 1e-4$, respectively. These figures show the existence of the boundary layer near $x = 1$. As the exact solution of the problem (6.2) is not known, to obtain the accuracy of the numerical solution and also to demonstrate the $\varepsilon-$uniform convergence of the proposed scheme, we use the double mesh principle which is given in the following. Let $\widetilde{U}^{2N,\Delta t/4}(x_i,t_n)$ be the numerical solution obtained on the fine mesh $\widetilde{G}_{\varepsilon}^{2N,4M} = \overline{\Omega}_x^{2N} \times S_t^{4M}$ with $2N$ mesh intervals in the spatial direction and $4M$ mesh intervals in the $t-$direction. Then for each ε, we calculate the maximum point-wise error by

$$E_{\varepsilon}^{N,\Delta t} = \max_{(x_i,t_n)\in\overline{G}_{\varepsilon}^{N,M}} \left| U^{N,\Delta t}(x_i,t_n) - \widetilde{U}^{2N,\Delta t/4}(x_i,t_n) \right|,$$

and the corresponding order of convergence by

$$P_{\varepsilon}^{N,\Delta t} = \log_2 \left(\frac{E_{\varepsilon}^{N,\Delta t}}{E_{\varepsilon}^{2N,\Delta t/4}} \right).$$

Table 3: *Maximum point-wise error of the normalized flux* $r_\varepsilon^{N,\Delta t}$ *for Example* 6.1.

	Number of Intervals N					
ε	32	64	128	256	512	1024
10^0	5.3355e-02	2.7699e-02	1.3932e-02	6.9761e-03	3.4893e-03	1.7448e-03
10^{-2}	8.7792e-02	4.3418e-02	2.1557e-02	1.0736e-02	5.3570e-03	2.6756e-03
10^{-4}	9.6645e-02	4.6782e-02	2.3437e-02	1.2285e-02	5.9339e-03	2.9212e-03
10^{-6}	1.0178e-01	4.8033e-02	2.3727e-02	1.1715e-02	5.8266e-03	2.9129e-03
10^{-8}	9.9448e-02	5.0228e-02	2.4087e-02	1.1768e-02	5.8576e-03	2.9163e-03
10^{-10}	1.0395e-01	5.3663e-02	2.4445e-02	1.2024e-02	5.8370e-03	2.9196e-03

Table 4: *Rate of convergence of the normalized flux* $q_\varepsilon^{N,\Delta t}$ *for Example* 6.1.

	Number of Intervals N				
ε	32	64	128	256	512
10^0	0.9458	0.9914	0.9979	0.9995	0.9999
10^{-2}	1.0158	1.0101	1.0057	1.0030	1.0016
10^{-4}	1.0467	0.9972	0.9319	1.0498	1.0224
10^{-6}	1.0834	1.0175	1.0182	1.0076	1.0002
10^{-8}	0.9855	1.0602	1.0334	1.0065	1.0062
10^{-10}	0.9539	1.1344	1.0236	1.0426	0.9995

The calculated maximum point-wise errors $E_\varepsilon^{N,\Delta t}$ and the corresponding order of convergence $P_\varepsilon^{N,\Delta t}$ for Example 6.2 are given in Table 5 and Table 6 respectively. The numerical results given in these tables reveal the first-order convergence independent of the diffusion parameter ε.

Further, the errors in the normalized flux have been calculated as

$$R_\varepsilon^{N,\Delta t} = \max_{1\le n\le M} \|F_\varepsilon^N U^{N,\Delta t}(x_N,t_n) - F_\varepsilon^N \widetilde{U}^{2N,\Delta t/4}(x_N,t_n)\|,$$

and the rate of convergence is determined from

$$Q_\varepsilon^{N,\Delta t} = \log_2\left(\frac{R_\varepsilon^{N,\Delta t}}{R_\varepsilon^{2N,\Delta t/4}}\right).$$

The calculated maximum point-wise errors in the normalized flux $R_\varepsilon^{N,\Delta t}$ and the corresponding order of convergence $Q_\varepsilon^{N,\Delta t}$ for Example 6.2 are given in Table 7 and Table 8 respectively. The maximum pointwise errors are plotted in loglog scale in

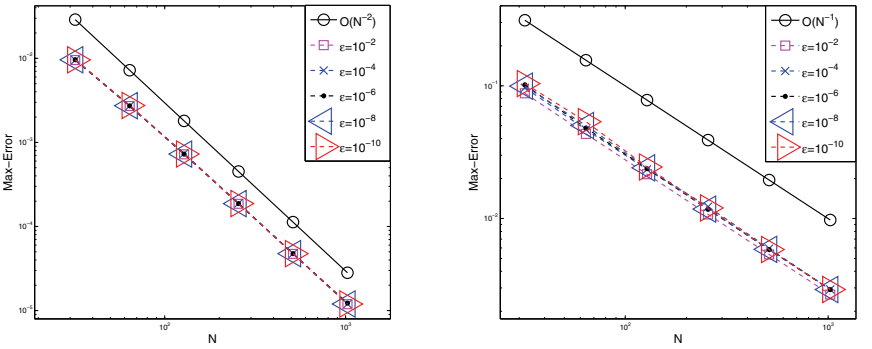

(a) Maximum point-wise error of the solution $e_\varepsilon^{N,\Delta t}$ (b) Maximum point-wise error of the normalized flux $r_\varepsilon^{N,\Delta t}$

Figure 1: Loglog plot for Example 6.1

Figures 3 (a) and (b), for the solution and the normalized flux, respectively. From these figures, one can easily observe the first-order ε–uniform convergence.

Table 5: *Maximum point-wise error of the solution* $E_\varepsilon^{N,\Delta t}$ *for Example* 6.2.

	Number of Intervals N				
ε	64	128	256	512	1024
10^{0}	1.0917e-02	3.8150e-03	1.0572e-03	2.7173e-04	6.8413e-05
10^{-2}	1.4096e-02	3.7384e-03	9.5054e-04	2.3869e-04	5.9756e-05
10^{-4}	1.3535e-02	3.6162e-03	9.4849e-04	2.3289e-04	5.8590e-05
10^{-6}	1.3226e-02	3.5997e-03	8.9781e-04	2.3232e-04	5.8252e-05
10^{-8}	1.3310e-02	3.5222e-03	9.0320e-04	2.3240e-04	5.8142e-05
10^{-10}	1.4050e-02	3.6114e-03	9.2446e-04	2.2594e-04	5.6480e-05

Example 6.3 *Consider the following quasilinear parabolic initial-boundary value problem:*

$$u_t(x,t) - \varepsilon u_{xx}(x,t) + \exp(u(x,t)) = f(x,t), \quad (x,t) \in (0,1)\times(0,1]. \tag{25}$$

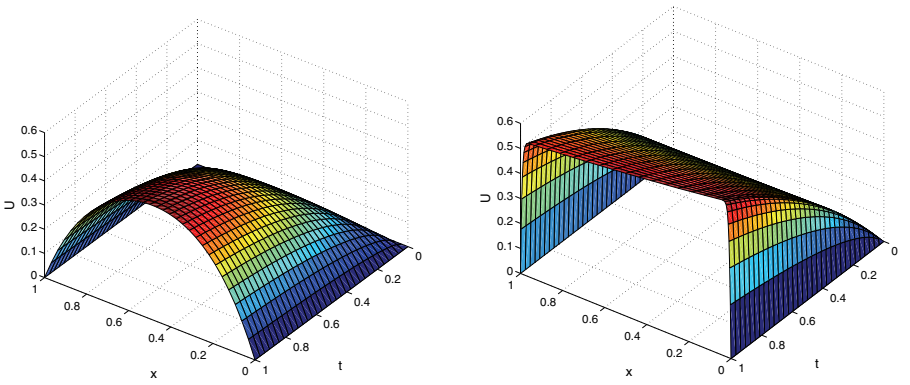

(a) $\varepsilon = 10^{-1}$ (b) $\varepsilon = 10^{-4}$

Figure 2: Numerical solution of Example 6.2 for $N = 32$ and $\Delta t = 1/32$.

Table 6: *Rate of convergence of the solution* $P_\varepsilon^{N,\Delta t}$ *for Example* 6.2.

	Number of Intervals N			
ε	64	128	256	512
10^{0}	1.5169	1.8515	1.9600	1.9898
10^{-2}	1.9148	1.9756	1.9936	1.9980
10^{-4}	1.9041	1.9308	2.0260	1.9909
10^{-6}	1.8775	2.0034	1.9503	1.9957
10^{-8}	1.9179	1.9634	1.9584	1.9989
10^{-10}	1.9599	1.9659	2.0327	2.0002

The right-hand side source term, initial and boundary conditions are calculated from the exact solution

$$u(x,t) = \left(t + \frac{x^2}{2\varepsilon}\right) \operatorname{erfc}\left(\frac{x}{2\sqrt{\varepsilon t}}\right) - \sqrt{\frac{t}{\pi\varepsilon}}\, x e^{-x^2/4\varepsilon t},$$

where erfc is the complementary error function.

If we use the Newton linearization process given in (21), we obtain the following system of linear singular perturbation parabolic PDEs:

Table 7: *Maximum point-wise error of the normalized flux* $R_{\varepsilon}^{N,\Delta t}$ *for Example* 6.2.

	Number of Intervals N				
ε	64	128	256	512	1024
10^{0}	4.0516e-02	1.5649e-02	7.4488e-03	3.7028e-03	1.8486e-03
10^{-2}	2.8779e-02	1.3846e-02	6.8861e-03	3.4549e-03	1.7334e-03
10^{-4}	2.4718e-02	1.1629e-02	5.3376e-03	2.9149e-03	1.5512e-03
10^{-6}	2.3159e-02	1.2046e-02	6.2308e-03	3.2183e-03	1.6336e-03
10^{-8}	2.2182e-02	1.1756e-02	6.1431e-03	3.2159e-03	1.6105e-03
10^{-10}	2.1247e-02	1.0875e-02	5.9366e-03	3.2089e-03	1.6278e-03

Table 8: *Rate of convergence of the normalized flux* $Q_{\varepsilon}^{N,\Delta t}$ *for Example* 6.2.

	Number of Intervals N			
ε	64	128	256	512
10^{0}	1.3724	1.0710	1.0084	1.0022
10^{-2}	1.0556	1.0077	0.9950	0.9950
10^{-4}	1.0879	1.1234	0.8727	0.9101
10^{-6}	0.9430	0.9511	0.9531	0.9782
10^{-8}	0.9160	0.9364	0.9337	0.9977
10^{-10}	0.9663	0.8733	0.8876	0.9791

$$\begin{cases} u_t^{m+1} - \varepsilon u_{xx}^{m+1} + (1+x(1-x))u_x^{m+1} + \exp(u^m)u^{m+1} = f(x,t) - \exp(u^m)(1-u^m), \\ u^{m+1}(x,0) = u(x,0), \quad 0 < x < 1, \\ u^{m+1}(0,t) = u(0,t), \quad u^{m+1}(1,t) = u(1,t), \quad 0 \le t \le 1. \end{cases} \tag{26}$$

Hence for fixed m, we solve (26) using computation methods discussed earlier. Once we get the prescribed tolerance bound we terminate the Newton Sequence and take that as the solution to the problem.

As the exact solution of the problem (6.3) is known, for each ε, we calculate the maximum point-wise error by

$$\tilde{e}_{\varepsilon}^{N,\Delta t} = \max_{(x_i,t_n)\in\overline{G}_{\varepsilon}^{N,M}} |u(x_i,t_n) - U^{N,\Delta t}(x_i,t_n)|,$$

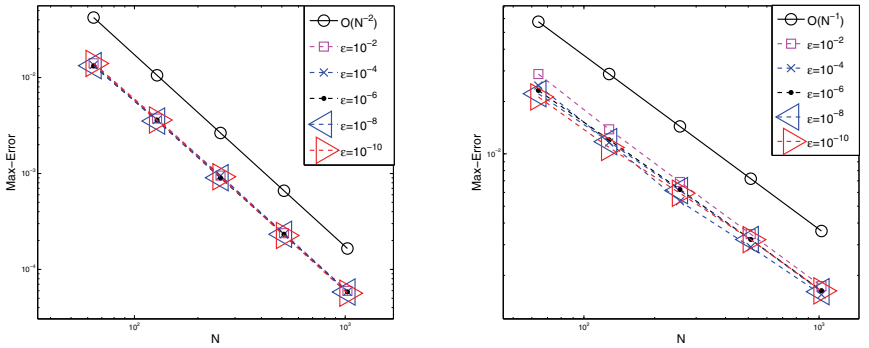

(a) Maximum point-wise error of the solution $E_\varepsilon^{N,\Delta t}$ (b) Maximum point-wise error of the normalized flux $R_\varepsilon^{N,\Delta t}$

Figure 3: Loglog plot for Example 6.2

Table 9: *Maximum point-wise error of the solution* $\tilde{e}_\varepsilon^{N,\Delta t}$ *for Example* 6.3.

	Number of Intervals N					
ε	32	64	128	256	512	1024
10^{0}	8.3530e-03	2.6259e-03	7.1230e-04	1.8369e-04	4.6626e-05	1.1745e-05
10^{-2}	9.5058e-03	2.7076e-03	7.2145e-04	1.8605e-04	4.7250e-05	1.1905e-05
10^{-4}	9.4968e-03	2.7178e-03	7.3745e-04	1.8835e-04	4.7626e-05	1.1983e-05
10^{-6}	9.5866e-03	2.7136e-03	7.2560e-04	1.8717e-04	4.7525e-05	1.2264e-05
10^{-8}	9.5733e-03	2.7296e-03	7.2625e-04	1.8722e-04	4.7546e-05	1.1978e-05
10^{-10}	9.5725e-03	2.7475e-03	7.2749e-04	1.8754e-04	4.7531e-05	1.1979e-05

where $u(x_i,t_n)$ and $U^{N,\Delta t}(x_i,t_n)$ respectively, denote the exact and the numerical solution obtained on the mesh with N mesh intervals in the spatial direction and M mesh intervals in the $t-$direction such that $\Delta t = T/M$ is the uniform time step. In addition, we determine the corresponding order of convergence by

$$\tilde{p}_\varepsilon^{N,\Delta t} = \log_2\left(\frac{\tilde{e}_\varepsilon^{N,\Delta t}}{\tilde{e}_\varepsilon^{2N,\Delta t/4}}\right).$$

The calculated maximum point-wise errors $\tilde{e}_\varepsilon^{N,\Delta t}$ and the corresponding order of convergence $\tilde{p}_\varepsilon^{N,\Delta t}$ for Example 6.3 are given in Table 9 and Table 10 respectively. From these results one can observe the ε–uniform first-order convergence of the numerical solution.

Table 10: *Rate of convergence of the solution* $\tilde{p}_{\varepsilon}^{N,\Delta t}$ *for Example* 6.3 .

	Number of Intervals N				
ε	32	64	128	256	512
10^{0}	1.6695	1.8822	1.9553	1.9780	1.9891
10^{-2}	1.8118	1.9080	1.9552	1.9773	1.9887
10^{-4}	1.8050	1.8818	1.9691	1.9836	1.9907
10^{-6}	1.8208	1.9030	1.9549	1.9776	1.9542
10^{-8}	1.8103	1.9101	1.9558	1.9773	1.9889
10^{-10}	1.8007	1.9172	1.9557	1.9802	1.9883

Table 11: *Maximum point-wise error of the normalized flux* $\tilde{r}_{\varepsilon}^{N,\Delta t}$ *for Example* 6.3.

	Number of Intervals N					
ε	32	64	128	256	512	1024
10^{0}	2.2918e-02	1.2507e-02	6.3366e-03	3.1787e-03	1.5906e-03	7.9548e-04
10^{-2}	4.3572e-02	2.2997e-02	1.1821e-02	5.9944e-03	3.0187e-03	1.5148e-03
10^{-4}	5.3688e-02	2.6997e-02	1.7934e-02	7.8518e-03	3.7102e-03	1.8090e-03
10^{-6}	6.0318e-02	2.8525e-02	1.4424e-02	7.1679e-03	3.5816e-03	2.5805e-03
10^{-8}	5.7455e-02	3.1194e-02	1.4862e-02	7.2315e-03	3.6193e-03	1.8034e-03
10^{-10}	6.2618e-02	3.5452e-02	1.5299e-02	7.5450e-03	3.5942e-03	1.8074e-03

The errors in the normalized flux have been calculated as

$$\tilde{r}_{\varepsilon}^{N,\Delta t} = \max_{1\le n\le M} \|F_{\varepsilon}u(x_0,t_n) - F_{\varepsilon}^{N}U^{N,\Delta t}(x_0,t_n)\|,$$

and the rate of convergence is determined from

$$\tilde{q}_{\varepsilon}^{N,\Delta t} = \log_2\left(\frac{\tilde{r}_{\varepsilon}^{N,\Delta t}}{\tilde{r}_{\varepsilon}^{2N,\Delta t/4}}\right).$$

The calculated maximum point-wise errors in the normalized flux $\tilde{r}_{\varepsilon}^{N,\Delta t}$ and the corresponding order of convergence $\tilde{q}_{\varepsilon}^{N,\Delta t}$ for Example 6.3 are given in Table 11 and Table 12. Again, one can see the ε–uniform convergence in Table 11, and the first-order convergence rate from Table 12.

7 Conclusions

In this article, we solved the singularly perturbed time-dependent reaction-diffusion problems (1) numerically by the upwind finite difference scheme on layer adapted

Table 12: *Rate of convergence of the normalized flux* $\tilde{q}_{\varepsilon}^{N,\Delta t}$ *for Example* 6.3.

	Number of Intervals N				
ε	32	64	128	256	512
10^{0}	0.8737	0.9810	0.9953	0.9988	0.9997
10^{-2}	0.9219	0.9602	0.9796	0.9897	0.9948
10^{-4}	0.9918	0.5901	1.1916	1.0815	1.0363
10^{-6}	1.0804	0.9837	1.0089	1.0010	0.4729
10^{-8}	0.8812	1.0696	1.0393	0.9986	1.0050
10^{-10}	0.8207	1.2124	1.0199	1.0698	0.9918

nonuniform grids obtained equdistributing the monitor function given in (8). The truncation error and stability analysis are obtained. The proposed numerical scheme is of first-order in temporal and second-order in spacial variables, *i.e.*, $O(\Delta t + N^{-2})$. Error estimates are derived for the numerical scheme, which are independent of the diffusion parameter ε. Numerical results reveal the theoretical error estimate.

References

Beckett, G.; Mackenzie, J. A. (2001): On a uniformly accurate finite difference approximation of a singularly perturbed reaction-diffusion problem using grid equidistribution. *J. Comput. Appl. Math.*, vol. **131**, pp. 381–405.

Beckett, G.; Mackenzie, J. A. (2000): Convergence analysis of finite difference approximations on equidistributed grids to a singularly perturbed boundary value problem. *Appl. Numer. Math.*, vol. **35(2)**, pp. 87–109.

Deb, R.; Natesan, S. (2009): Higher-order time accurate numerical methods for singularly perturbed parabolic partial differential equations. *Int. J. Comput. Math.*, vol. **86(7)** , pp. 1204–1214.

Deb, B.S.; Natesan, S. (2008): Richardson Extrapolation Method for Singularly Perturbed Coupled System of Convection-Diffusion Boundary-Value Problems. *CMES: Computer Modeling in Engineering & Sciences*, vol. **38(2)**, pp. 179–200.

Ewing, R.E. (1983): The Mathematics of Reservoir Simulation. *SIAM*, Philadelphia.

Farrell, P.A.; Hegarty, A.F.; Miller, J.J.H.; O'Riordan, E.; Shishkin, G.I. (2000): Robust Computational Techniques for Boundary Layers. *Chapman & Hall/CRC Press*.

Farrell, P.A.; Hemker, P.W.; Shishkin, G.I. (1996): Discrete approximations for singularly perturbed boundary value problems with parabolic layers. *J. Comp. Math.*, vol. **14** , pp. 71–97.

Guo, W.; Stynes, M. (1993): Finite element analysis of exponentially fitted lumped schemes for time-dependent convection-diffusion problems. *Numer. Math.*, vol. **66** , pp. 347–371.

Kellogg, R.B.; Tsan, A. (1978): Analysis of some differences approximations for a singular perturbation problem without turning point. *Math. Comp.*, vol. **32**, pp. 1025–1039.

Ladyženskaja, O.A.; Solonnikov, V.A.; Ural'ceva, N.N. (1988): Linear and Quasi-linear Equations of Parabolic Type. *American Mathematical Society Providence, Rhode Island*.

Liu, C.-S. (2006): The Lie-group shooting method for singularly perturbed two-point boundary-value problems. *CMES: Computer Modeling in Engineering & Sciences*, vol. **15**, pp. 179–196.

Miller, J.J.H.; O'Riordan, E.; Shishkin, G.I. (1996): Fitted Numerical Methods for Singular Perturbation Problems. *World Scientific, Singapore, 1996*.

Miller, J.J.H.; O'Riordan, E.; Shishkin, G.I.; Sishkina, L.P. (1998): Fitted mesh methods for problems with parabolic boundary layers. *Math. Proc. R. Ir. Acad.*, vol. **98A** , pp. 173–190.

Mukherjee, K.; Natesan, S. (2008): An Efficient Numerical Scheme for Singularly Perturbed Parabolic Problems with Interior Layer. *Neural, Parallel, and Scientific Computations*, vol. **16**, pp. 405–418.

Natesan, S.; Deb, R. (2008): A robust numerical scheme for singularly perturbed parabolic reaction-diffusion problems. *Neural, Parallel, and Scientific Computations*, vol. **16**, pp. 419-434.

Roos, H.-G.; Stynes, M.; Tobiska, L. (2006): Numerical Methods for Singularly Perturbed Differential Equations. *Springer, Berlin*.

Shishkin, G.I. (1989): Approximation of solutions of singularly perturbed boundary value problems with a parabolic layer. *USSR Comput. Maths. Math. Phys.*, vol. **29**, pp. 1–10.

Stynes, M.; O'Riordan, E. (1989): Uniformly convergent difference schemes for singularly perturbed parabolic diffusion-convection problems without turning points. *Numer. Math.*, vol. **55**, pp. 521–544.